J. Biochem. 2010;147(3):337–344 doi:10.1093/jb/mvp170

JB THE JOURNAL OF BIOCHEMISTRY

Role of *N*-glycans in maintaining the activity of protein *O*-mannosyltransferases POMT1 and POMT2

Received September 18, 2009; accepted October 13, 2009; published online October 29, 2009

Hiroshi Manya[1,*], Keiko Akasaka-Manya[1], Ai Nakajima[1,2], Masao Kawakita[2] and Tamao Endo[1]

[1]Glycobiology Research Group, Tokyo Metropolitan Institute of Gerontology, Foundation for Research on Aging and Promotion of Human Welfare, 35-2 Sakaecho, Itabashi-ku, Tokyo 173-0015; and [2]Department of Applied Chemistry, Kogakuin University, Tokyo 163-8677, Japan

*Hiroshi Manya. Glycobiology Research Group, Tokyo Metropolitan Institute of Gerontology, Foundation for Research on Aging and Promotion of Human Welfare, 35-2 Sakaecho, Itabashi-ku, Tokyo 173-0015, Japan, Tel: 81-3-3964-3241, Ext. 3055, Fax: 81-3-3579-4776, E-mail: manya@tmig.or.jp.

The complex of protein *O*-mannosyltransferase 1 (POMT1) and POMT2 catalyzes the initial step of *O*-mannosyl glycan biosynthesis. The mutations in either *POMT1* or *POMT2* can lead to Walker–Warburg syndrome, a congenital muscular dystrophy with abnormal neuronal migration. Here, we used three algorithms for predicting transmembrane helices to construct the secondary structural models of human POMT1 and POMT2. In these models, POMT1 and POMT2 have seven- and nine-transmembrane helices and contain four and five potential *N*-glycosylation sites, respectively. To determine whether these sites are actually glycosylated, we prepared mutant proteins that were defective in each site by site-directed mutagenesis. Three of the POMT1 sites and all of the POMT2 sites were found to be *N*-glycosylated, suggesting that these sites face the luminal side of the endoplasmic reticulum. Mutation of any single site did not significantly affect POMT activity, but mutations of all *N*-glycosylation sites of either POMT1 or POMT2 caused a loss of POMT activity. The loss of activity appeared to be due to the decreased hydrophilicity. These results suggest that the *N*-glycosylation of POMT1 and POMT2 is required for maintaining the conformation as well as the activity of the POMT1-POMT2 complex.

Keywords: *N*-glycosylation/protein *O*-mannosyltransferase/POMT1/POMT2/secondary structure.

Abbreviations: α-DG, α-Dystroglycan; Dol-P-Man, dolichyl phosphate mannose; ER, endoplasmic reticulum; Man, mannose; SDS–PAGE, sodium dodecyl sulfate-polyacrylamide gel electrophoresis; WWS, Walker–Warburg syndrome; POMT1, protein *O*-mannosyltransferase 1; POMT2, protein *O*-mannosyltransferase 2; HEK, Human embryonic kidney.

Protein *O*-mannosyltransferase 1 (POMT1) and POMT2 (POMT, EC 2.4.1.109), which are located in the endoplasmic reticulum (ER) membrane, catalyze the initial step of *O*-mannosyl glycans biosynthesis, *i.e.* the transfer of a mannosyl residue from dolichyl phosphate mannose (Man) (Dol-P-Man) to Ser/Thr residues of certain proteins (*1*). Mutations in *POMT1* and *POMT2* are reported to cause Walker–Warburg syndrome (WWS: OMIM 236670), an autosomal recessive developmental disorder associated with congenital muscular dystrophy, neuronal migration defects and ocular abnormalities (*2*, *3*). Previously, we found that α-dystroglycan (α-DG) was predominantly modified by *O*-mannosyl glycans, Siaα2-3Galβ1-4GlcNAcβ1-2Man (*4*), and reported that defects in *O*-mannosyl glycan on α-DG cause several α-dystroglycanopathies, which are a group of congenital muscular dystrophies that include WWS, muscle–eye–brain disease (MEB: OMIM 253280) and Fukuyama congenital muscular dystrophy (FCMD: OMIM 253800) (*5*, *6*). α-DG is a component of the dystrophin–glycoprotein complex that acts as a transmembrane linker between the extracellular matrix and intracellular cytoskeleton (*7*). *O*-Mannosyl glycans of α-DG have a role in binding to extracellular matrixes such as laminin, neurexin and agrin (*4*, *8–11*). When α-DG fails to bind to laminin or other molecules in the extracellular matrix as a result of a defect in α-DG glycosylation, it is thought to interrupt normal muscular function and migration of neurons in the developing brain (*12*). Thus, *O*-mannosyl glycans are indispensable for normal structure and function of α-DG in muscle and brain.

Several mutations in the *POMT1* and *POMT2* genes were identified in patients with WWS (*2*, *3*, *13*). We previously demonstrated that these mutations lead to defects of POMT activity (*13*, *14*). We also confirmed that formation of a complex of POMT1 and POMT2 was required for POMT activity (*15*). However, the mechanism(s) by which the mutations cause a loss of POMT activity and the significance of complex formation remain unclear. POMT1 and POMT2 are homologous to protein *O*-mannosyltransferases (PMTs) in yeast. *Saccharomyces cerevisiae* has seven pmts (pmt1–7) that form hetero and homo complexes in various combinations (*16*). Yeast pmt1 has been proposed to consist of seven transmembrane helices (*17*). The pmt1 N-terminus and loops 2, 4 and 6 are located in the cytoplasm, and the C-terminus and loops 1, 3 and 5 are located in the ER lumen. A large hydrophilic region (loop 5) and loop 1 have been reported to be important for enzymatic activity (*17–19*).

Glycoprotein glycans strongly affect various biological and physical properties of proteins, such as their stabilities, conformations, interactions, cellular localizations and trafficking. The presence or absence of *N*-glycans in PMTs, as well as their structures and roles has not yet been ascertained. Human POMT1 and POMT2 contain four and five potential *N*-glycosylation sites, respectively. In the present study, we used three algorithms for predicting transmembrane helices to construct models of the secondary structures of human POMT1 and POMT2, and determined the topology of both POMTs by analyzing the *N*-glycosylation status of potential site. Furthermore, by removing potential *N*-glycosylation sites, we showed that the *N*-glycans are required for POMT activity.

Materials and methods

Vector construction of POMT1 and POMT2 mutants

cDNAs for the most common splicing variant of human myc-tagged *POMT1* (lacking bases 700–765, corresponding to amino acids 234–255) and non-tagged *POMT2* were used for site-directed mutagenesis and cloned into pcDNA 3.1 (Invitrogen Corp., Carlsbad, CA, USA), as described previously (*15*). The *POMT1* and *POMT2* genes were modified with a QuickChange Site-Directed Mutagenesis Kit (STRATAGENE, La Jolla, CA, USA) according to the manufacturer's instructions. All mutant clones were sequenced to confirm the presence of the mutations. The primer pairs used to make the mutants were: N16Q, 5′-GTGACGGCTGACATCCAATTGAGCCTTGTGGCC-3′ and 5′-GGCCACAAGGCTCAATTGGATGTCAGCCGTCAC-3′; N435Q, 5′-CCTGCTACATTGACTATCAAATCTCCATGCCCGCCC-3′ and 5′-CCTGCTACATTGACTATCAAATCTCCATGCCCGCCC-3′; N471Q, 5′-GTCCGCTTTGTGCACGTGCAAACTTCCGCTGTC-3′ and 5′-GACAGCGGAAGTTTGCACGTGCACAAAGCGGAC-3′; N539Q, 5′-GGTGGACGTCAGCAGGCAACTCAGCTTCATGG-3′ and 5′-CCATGAAGCTGAGTTGCCTGCTGACGTCCACC-3′; N98Q, 5′-GTTACTATATCCAACGTACATTTTTCTTTGATGTGCACCCGCC-3′ and 5′-GGCGGGTGCACATCAAAGAAAAATGTACGTTGGATATAGTAAC-3′; N330Q, 5′-CAGGGAACAACCTGCACCAAGCTTCCATCCCTG-3′ and 5′-CAGGGATGGAAGCTTGGTGCAGGTTGTTCCCTG-3′; N445Q, 5′-GGTCACCGGATATGGCATACAAGGAACAGGGGAC-3′ and 5′-GTCCCCTGTTCCTTGTATGCCATATCCGGTGACC-3′; N528Q, 5′-CCCAAGTTGCCACAAATCAGCCTGGATGTGCTACAG-3′ and 5′-CTGTAGCACATCCAGGCTGATTTGTGGCAACTTGGG-3′; N583Q, 5′-CGCTTCTCAGGGGTCCAAGACACAGATTTCCGAG-3′ and 5′-CTCGGAAATCTGTGTCTTGGACCCCTGAGAAGCG-3′.

Expression of POMTs and preparation of microsomal fraction

Human embryonic kidney (HEK) 293T cells were maintained in Dulbecco's modified Eagle's medium (Invitrogen) supplemented with 10% fetal bovine serum, 2 mM L-glutamine, 100 units/ml penicillin and 50 μg/ml streptomycin at 37°C with 5% CO_2. Expression plasmids were transfected into HEK293T cells using Lipofectamine Plus reagent (Invitrogen) according to the manufacturer's instructions. Cells were incubated for 3 days to produce POMT1 and POMT2 proteins. The cells were homogenized in 10 mM Tris–HCl, pH 7.4, 1 mM EDTA, 250 mM sucrose, 1 mM DTT, with protease inhibitor mixture (3 μg/ml pepstatin A, 1 μg/ml leupeptin, 1 mM benzamidine-HCl, 1 mM PMSF). After centrifugation at 900*g* for 10 min, the supernatant was subjected to ultracentrifugation at 100,000*g* for 1 h. The precipitate was used as the microsomal fraction. Protein concentration was determined by BCA assay (Thermo Fisher Scientific Inc., Waltham, MA, USA). Microsomal fractions were solubilized with 20 mM Tris–HCl, pH 8.0, 2 mM 2-mercaptoethanol, 10 mM EDTA and 0.5% *n*-octyl-β-D-thioglucoside at 4°C. After centrifugation at 10,000*g* for 10 min, the supernatant was used as solubilized supernatant.

To examine the effects of tunicamycin, tunicamycin was added to the culture medium after transfection at a final concentration of 1 μg/ml, and the culture was continued for 3 days. A microsomal fraction and a solubilized microsomal fraction were obtained as described earlier.

Western blot analysis

The microsomal fractions (20 μg) or solubilized supernatants were separated by sodium dodecyl sulfate-polyacrylamide gel electrophoresis (SDS–PAGE) (7.5% gel) and proteins were transferred to a polyvinylidene difluoride membrane. The membrane was blocked in PBS containing 5% skim milk and 0.05% Tween 20, incubated with anti-myc (A-14) antibody (Santa Cruz Biotech, Santa Cruz, CA, USA) or anti-POMT2 polyclonal antibody (*15*), and treated with anti-goat IgG conjugated with HRP (Santa Cruz Biotech) or anti-rabbit IgG conjugated with horseradish peroxidase (HRP) (GE Healthcare Bio-sciences Corp., Piscataway, NJ, USA). Proteins that bound to the antibody were visualized with an ECL kit (GE Healthcare Bio-sciences). As reported previously (*15*), anti-POMT2 antibody did not detect endogenous POMT2 but was specific to recombinant POMT2.

Assay for POMT activity

POMT activity was based on the amount of [^{3}H]-mannose transferred to a glutathione-S-transferase fusion α-dystroglycan (GST-α-DG) as described previously (*1*). The reaction mixture contained 20 mM Tris–HCl (pH 8.0), 100 nM of [^{3}H]-mannosylphosphoryldolichol (Dol-P-Man, 125,000 dpm/pmol) (American Radiolabeled Chemical, Inc., St Louis, MO, USA), 2 mM 2-mercaptoethanol, 10 mM EDTA, 0.5% *n*-octyl-β-D-thioglucoside, 10 μg GST-α-DG and enzyme source (80 μg of microsomal membrane fraction) in 20 μl total volume. After 1 h incubation at 22°C, the reaction was stopped by adding 150 μl PBS containing 1% Triton X-100 (Nacalai Tesque, Kyoto, Japan), and the reaction mixture was centrifuged at 10,000g for 10 min. The supernatant was removed, mixed with 400 μl of PBS containing 1% Triton X-100 and 10 μl of Glutathione-Sepharose 4B beads (GE Healthcare Bio-sciences), rotated at 4°C for 1 h, and washed three times with 20 mM Tris–HCl (pH 7.4) containing 0.5% Triton X-100. The radioactivity adsorbed to the beads was measured using a liquid scintillation counter.

Endo-glycosidase digestion

N-glycosidase F (PNGase F) and endoglycosidase H (Endo H) were purchased from Roche Diagnostics K.K. (Basel, Switzerland). The microsomal fraction (100 μg) was denatured with boiling for 3 min in denaturation buffer (40 μl) containing 0.1 M citrate-phosphate buffer containing 0.1% SDS, 20 mM EDTA and 10 mM 2-mercaptoethanol. After the mixture was cooled, 40 μl dilution buffer containing 0.1 M citrate-phosphate buffer and 2 U of PNGase F or 0.01 U of Endo H were added. The mixture was incubated at 37°C for 6 h. The pH values of the citrate-phosphate buffers were 7.0 for PNGase F or 5.5 for Endo H.

Results

Transmembrane prediction of human POMT1 and POMT2

The yeast *O*-mannosyltransferase pmt1 is proposed to have seven-transmembrane helices (*17*). In this study, the transmembrane topologies of human POMT1 and POMT2 were predicted with three algorithms specifically designed to detect transmembrane alpha helices: SOSUI (*20*), TMPred (*21*) and HMMTOP (*22*). The helices predicted by the three algorithms are shown by the colored underlines in Fig. 1, and as the consensus helices are highlighted in yellow. These results suggest that POMT1 and POMT2 have seven and nine transmembrane helices, respectively.

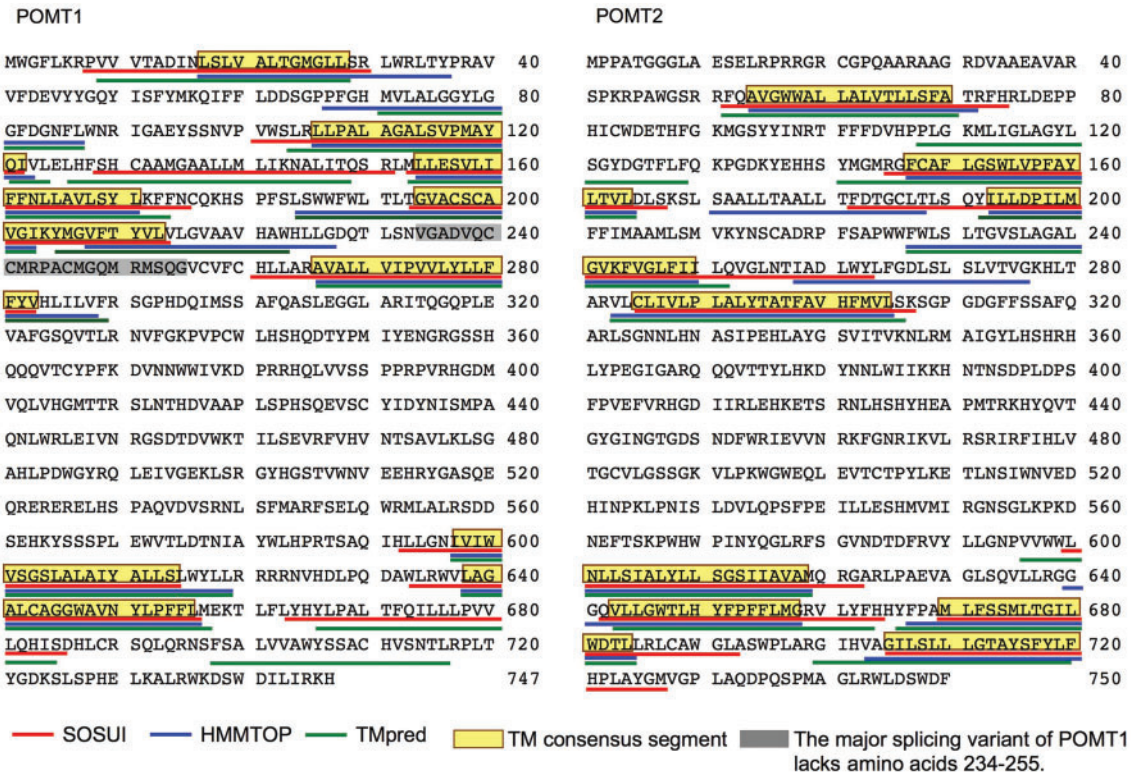

Fig. 1 Analysis of secondary structures of human POMT1 and POMT2. The secondary structure was predicted using three algorithms specifically designed to detect transmembrane alpha helices: SOSUI, TMPred and HMMTOP. The consensus segments predicted by three different algorithms were defined as the transmembrane segments: Amino acids of 17–28, 106–122, 154–171, 194–213, 266–283, 597–614 and 638–656 of human POMT1; amino acids of 54–70, 147–164, 193–210, 241–250, 285–295, 601–619, 643–658, 670–684 and 705–720 of human POMT2.

Transmembrane topologies of POMT1 and POMT2 by analysis of N-glycosylation site occupancy

The results of Fig. 1 suggest that each of POMT1 and POMT2 have two possible membrane topologies: the N-termini of POMT1 and POMT2 are on the cytosolic or luminal sides of the ER membrane or they are on the same side (Fig. 2A and B). Because *N*-glycosylation occurs only on the ER luminal side, it is possible to determine the correct topology by examining the *N*-glycosylated status of each protein. Human POMT1 and POMT2 have four (Asn^{16}, Asn^{435}, Asn^{471} and Asn^{539}) and five (Asn^{98}, Asn^{330}, Asn^{445}, Asn^{528} and Asn^{583}) potential *N*-glycosylation sites, respectively. If the N-terminus of POMT1 is on the cytosolic side, Asn^{16} would be predicted to be on the cytosolic side and Asn^{435}, Asn^{471} and Asn^{539} would be predicted to be on the luminal side. In this case, Asn^{435}, Asn^{471} and Asn^{539} could be *N*-glycosylated. On the other hand, if the N-terminus of POMT1 is on the luminal side, only Asn^{16} could be *N*-glycosylated. In the case of POMT2, if the N-terminus is on the cytosolic side, all five Asns (Asn^{98}, Asn^{330}, Asn^{445}, Asn^{528} and Asn^{583}) could be *N*-glycosylated, while if it on the luminal side, none could be *N*-glycosylated.

To determine the occupancy of each potential *N*-glycosylation site, we constructed expression vectors in which the Asn residue of each site was substituted by Gln (Fig. 2C) and transfected them into HEK293 cells. Fig. 3A shows a western blot analysis of six cell cultures, each doubly transfected with wild-type POMT2 and one of the POMT1 variants. Three of the mutant POMT1s (N435Q, N471Q and N539Q) (upper panel) were 2–3 kDa smaller than the wild type, a value corresponding to a single *N*-glycan chain. Only the N16Q mutant had the same molecular mass as the wild-type protein. The POMT2 sizes (lower panel) were unaffected, as expected. Similarly, Fig. 3B shows the sizes of POMT1 and POMT2 in cells doubly transfected with wild-type POMT1 and one of the POMT2 variants. All five of the POMT2 mutants were also 2–3 kDa smaller than the wildtype (lower panel), while POMT1 sizes (upper panel) were unaffected, as expected. When each mutant and wild counterpart was expressed in the presence of tunicamycin, an inhibitor of initiation of *N*-glycosylation, all expressed POMTs had the same molecular mass (data not shown). These results demonstrate that all but one of the Asn residues of the potential *N*-glycosylation sites of POMT1 and POMT2 (the exception being Asn^{16} of POMT1) have an *N*-glycan. Because the glycosylated Asn residues must be on the luminal side, the N-termini of POMT1 and POMT2 must be on the cytosolic side of the ER membrane based on the proposed models shown in Fig. 2. It is noteworthy that Nilsson and von Heijine (*23*) reported that a potential *N*-glycosylation site needed to be a distance of 12–14 amino acid residues from the membrane to be modified actually. Thus, the proximity of Asn^{16} of POMT1 to the membrane may hamper the glycosylation.

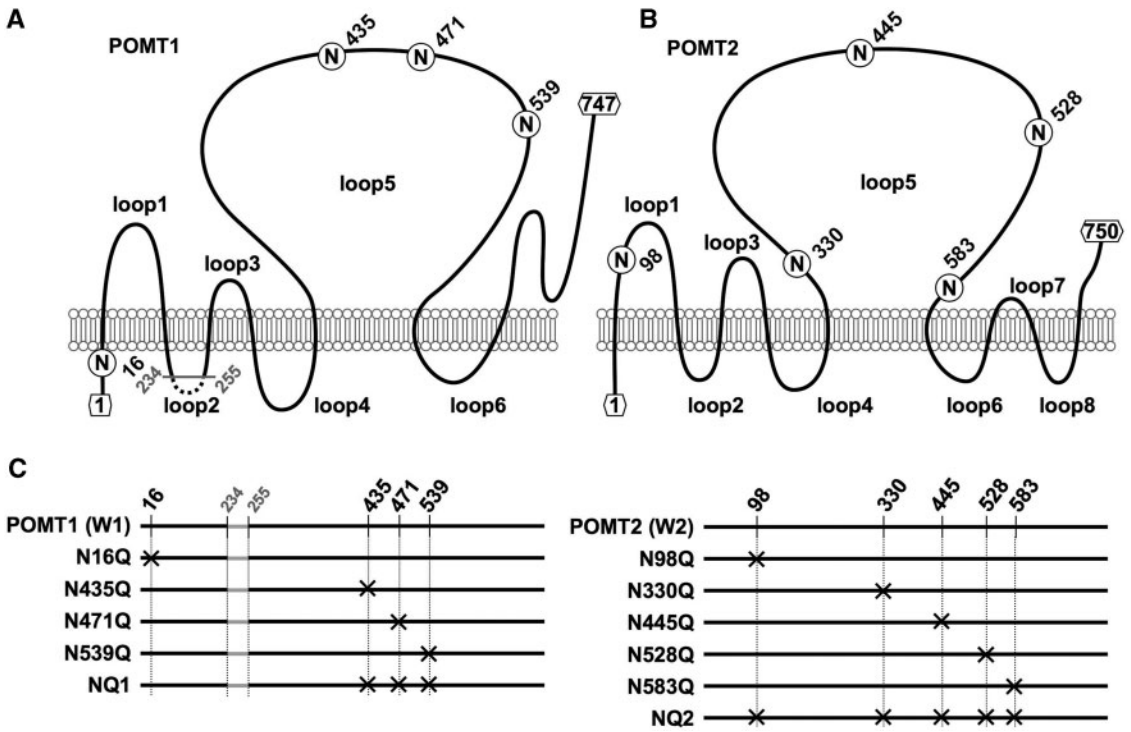

Fig. 2 Possible transmembrane topologies of human POMT1 and POMT2 (A and B), and a summary of mutations of potential *N*-glycosylation sites (C). The letters N (in circles) show Asn residues of potential *N*-glycosylation sites and the numbers indicate amino acid positions. The crosses in (C) indicate the substitution of Gln for Asn. The major splicing variant of POMT1, which lacks amino acids 234–255, was used in this study (*15*). Although the model does not specify which side of the ER membrane is the cytosolic side or luminal side, our conclusion is that the N-termini of POMT1 and POMT2 are on the cytosolic side of the ER membrane. There are possible other models; for example, some transmembrane helices in (A) and (B) may be non-transmembrane manner and be embedded in the membrane. However, after taking account of seven-transmembrane helices models of yeast pmt1 (*17*), two possible membrane topologies are shown here.

Together, further work is necessary to determine membrane topologies of POMT1 and POMT2 in the future.

Effect of N-glycosylation on POMT activity

To evaluate the contribution of the individual *N*-glycans on POMT1 and POMT2 to POMT activity, the POMT1 or POMT2 mutants were co-expressed with wild-type POMT2 (W2) or wild-type POMT1 (W1), respectively. As shown in Fig. 3C and D (hatched bars), POMT activity was significantly greater in all transfectants than in the mock transfectant. However, these activities were not accurate because the expression levels of each mutant protein were not equal as shown in Fig. 3A and B. Therefore, each activity was normalized to the amount of expressed protein. The individual *N*-glycosylation site mutations had comparable POMT activity to wildtype, except the N98Q transfectant showed a lower enzymatic activity to ~50% of wildtype, and N16Q, N435Q and N471Q transfectants did to ~70% of wildtype (Fig. 3C and D, closed bars).

Next, we generated the NQ1 and NQ2 mutants that have no *N*-glycans by substitution of Gln for Asn residues of all *N*-glycosylation sites of POMT1 and POMT2, respectively (Fig. 2C). These mutants and wild-type POMTs were co-expressed in the following combinations: W1 + W2, NQ1 + W2, W1 + NQ2 and NQ1 + NQ2. In the western blot analysis, NQ1 and NQ2 migrated faster than wild-type POMT1 and POMT2, respectively (Fig. 4A). As shown in Fig. 4B, the POMT activities of the microsomal fractions from three transfectants (NQ1 + W2, W1 + NQ2 and NQ1 + NQ2) were significantly lower than the activity of the W1 + W2 transfectant. These results clearly show that the *N*-glycans of both POMT1 and POMT2 are required for expression of POMT activity.

On the other hand, after the mock and W1 + W2 transfectants were cultured in media containing 1 μg/ml tunicamycin, W1 and W2 migrated to the same positions as NQ1 and NQ2 (Fig. 4A), respectively, on SDS-PAGE (Fig. 4C). As shown in Fig. 4D, the POMT activity of the microsomal fraction from [W1 + W2, TN(+)] was significantly lower than that from W1 + W2 without tunicamycin treatment [W1 + W2, TN(−)], indicating that the *N*-glycans of both POMT1 and POMT2 are required for POMT activity. Importantly, the POMT activities of the microsomal fractions from both tunicamycin-treated transfectants [Mock and W1 + W2, TN(+)] were strikingly decreased compared with the activity of the non-treated mock transfectant [Mock, TN(−)] (Fig. 4D). These results indicate that the inhibition of *N*-glycosylation by tunicamycin treatment inactivated not only the recombinant POMTs, but also the endogenous POMTs.

Role of N-glycosylation in solubility of POMTs

To understand why removing all the *N*-glycans on the POMT1 or POMT2 destroys POMT activity, we

assayed the solubility of the POMTs in a buffer containing 0.5% *n*-octyl-β-D-thioglucoside, which is the most effective detergent for measurement of POMT activity (*15*). As shown in Fig. 4E, POMT1 and POMT2 were detected in the solubilized supernatant from the W1 + W2 transfectant but not from the other transfectants. Similarly, neither POMT1 nor POMT2 was detected in the solubilized supernatant from the tunicamycin-treated W1 + W2 transfectant (Fig. 4F). The fact that neither POMT1 nor POMT2 was detected in the solubilized supernatant from NQ1 + W2 and W1 + NQ2 transfectants (Fig. 4E) demonstrates that the *N*-glycans of both POMT1 and POMT2 are necessary for solubilization of the POMT1–POMT2 complex. These results suggest that the inactivation of POMT was caused by the decreased hydrophilicity of proteins as a result of removing the *N*-glycans.

Endo-glycosidase treatment of POMTs

To elucidate the structures of the *N*-glycans on POMT1 and POMT2, W1 and W2 were treated with PNGase F and Endo H. As shown in Fig. 5, each glycosidase-treated W1 and W2 migrated to the same molecular mass as tunicamycin-treated POMT1 and POMT2, respectively, indicating that both PNGase F and Endo H digested all *N*-glycan chains on W1 and W2. Because Endo H preferentially cleaves high-Man type *N*-glycans (*24*, ,*25*), the *N*-glycans on both POMT1 and POMT2 were high-Man type. These results indicate that the POMT1 and POMT2 reside in the ER, and it is consistent with our previous report (*15*).

Discussion

In this study, we investigated the roles of *N*-glycans attached to human POMT1 and POMT2. The helical consensus regions (Fig. 1) indicate that POMT1 and POMT2 have seven- and nine-transmembrane domains, respectively. Human POMT1 and POMT2 contain four and five potential *N*-glycosylation sites, respectively, based on their amino acid sequences. Analysis of the sizes and activities of POMT mutants lacking single potential *N*-glycosylation sites by site-directed mutagenesis (Fig. 3) demonstrate that three sites of POMT1 (Asn^{435}, Asn^{471} and Asn^{539}) and five sites of POMT2 (Asn^{98}, Asn^{330}, Asn^{445} Asn^{528} and Asn^{583}) are glycosylated. The finding that only Asn^{16} of POMT1 was not glycosylated indicates that the glycosylated Asns are located in the ER lumen and that Asn^{16} is located in the cytosol. Any single *N*-glycan chain of POMT1 or POMT2 was dispensable for POMT activity, but the elimination of all *N*-glycans of either POMT1 or POMT2 inhibited POMT activity. The cause of inactivation of POMT has been the decreased hydrophilicity following the loss of the *N*-glycans. Together, these findings suggest that the *N*-glycosylation of POMTs is required to maintain the conformation and activity of the POMT1–POMT2 complex.

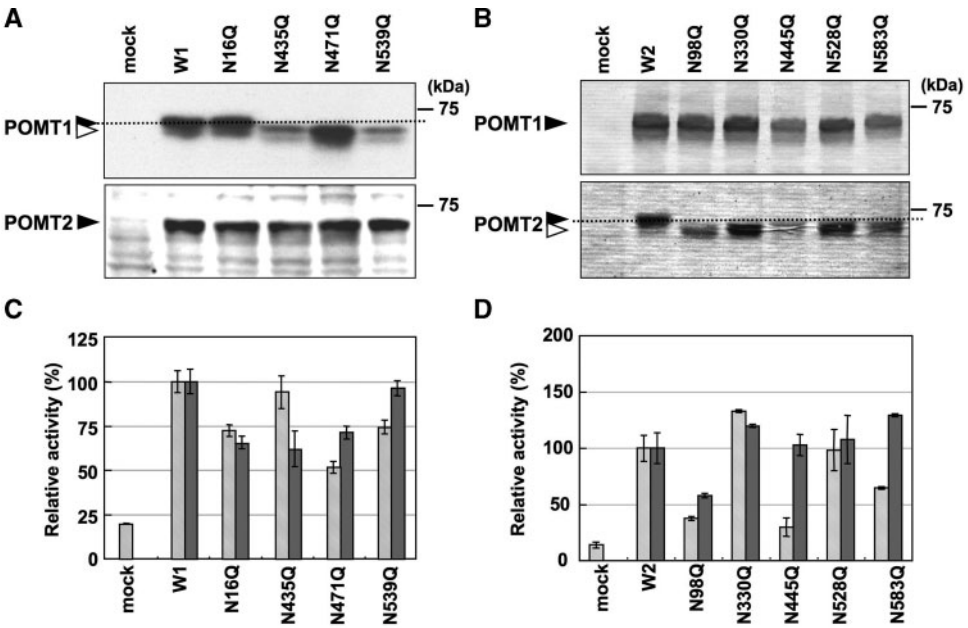

Fig. 3 Determination of the occupancy of the *N*-glycosylation sites on POMT1 and POMT2 and POMT activity of single *N*-glycosylation site mutants. (A) Western blot analyses of the microsomal fractions from the cells co-transfected with POMT1 mutants and W2. (B) W1 and POMT2 mutants. Closed triangles indicate the migration positions of fully glycosylated POMT1 and POMT2. Open triangles indicate the migration position of the mutant proteins, which lack single *N*-glycan chain. Molecular weight standards are shown on the right. The mock lanes were loaded with sample from cells transfected with vector only. The dotted lines of (A) and (B) show the migration position of fully glycosylated POMT1 and POMT2, respectively, for comparison with mutant proteins. The lower band of two bands detected by POMT1 western blots (by anti-myc antibody) was probably the degraded product. (C and D) POMT activities of the microsomal fractions obtained in (A) and (B). Hatched bars show total POMT activities in each microsomal fraction. The activity of mock lanes indicates endogenous POMT activity of HEK293 cells. Closed bars show the POMT activities corrected for expression levels of POMT1 and POMT2 proteins using NIH image. Average values ± SD of three independent experiments are shown.

Loop 5 of both POMT1 and POMT2, which are the largest hydrophilic regions formed on the luminal side, have amino acid sequences that are similar to the catalytic domains of yeast pmt1 (*17*, *19*) and thus are expected to be the catalytic domains of POMT1 and POMT2. Because the *N*-glycosylation sites are enriched on loop 5 (Fig. 2), it is possible that these *N*-glycans contribute to the hydrophilicity and affect the folding of the catalytic domain. The finding that removal of *N*-glycans from either POMT1 or POMT2 inhibited POMT activity (Fig. 4) suggests that loop 5 is required for the correct folding of the catalytic center in the POMT1–POMT2 complex. However, the *N*-glycans do not appear to be necessary for formation of the POMT1–POMT2 complex. This is because, when glycosylated and non-glycosylated combinations of POMT mutants (NQ1 + W2 and W1 + NQ2) were expressed in the same cells, neither protein was solubilized (Fig. 4), indicating the formation of a stable complex. A somewhat similar result was obtained with yeast Pmt1, in which deletion of loop 5 eliminated enzymatic activity, but did not

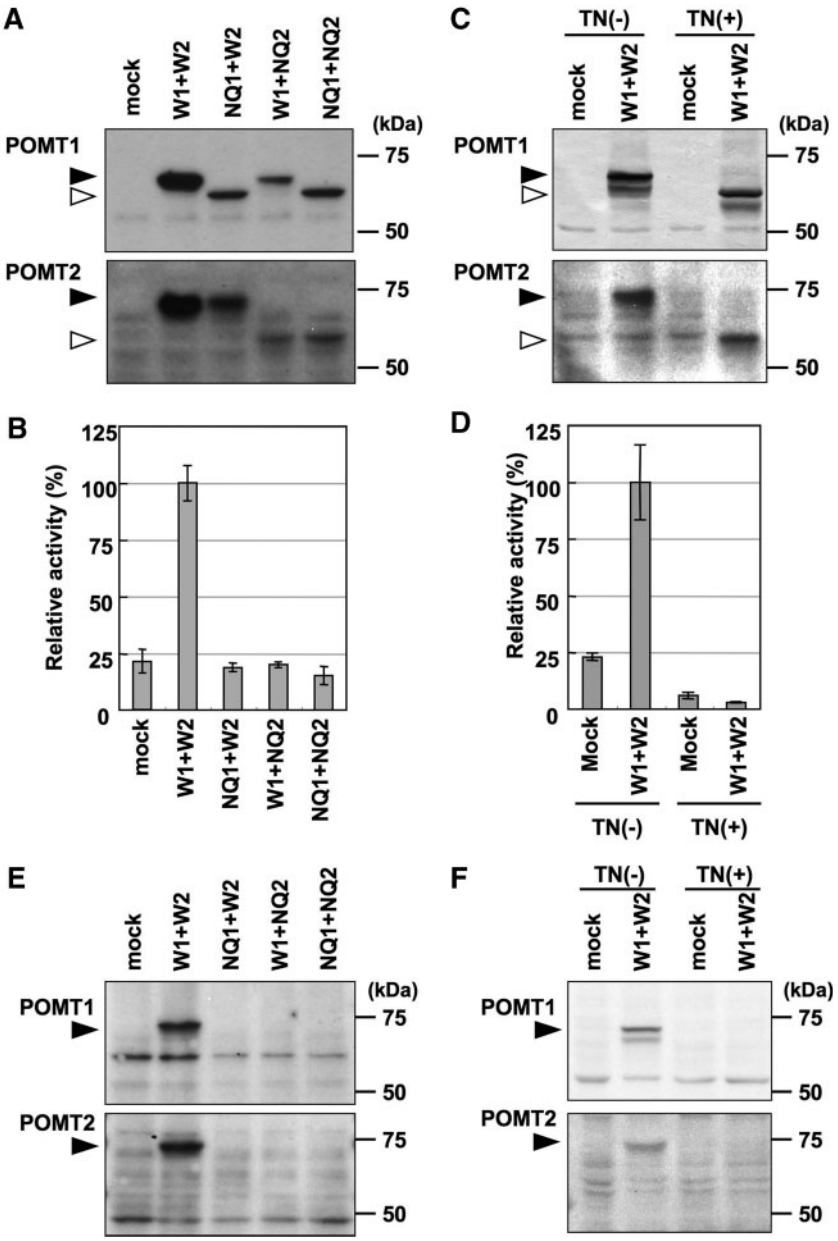

Fig. 4 Effect of *N*-glycan deficiency on POMT activity and on solubilization efficiency. (A and C) Western blot analyses of the microsomal fraction from cells expressing *N*-glycan-deficient mutants (A) and the W1 + W2 transfectants cultured with [TN(+)] or without tunicamycin [TN(−)] (C). (B and D) POMT activities of the microsomal fraction obtained in (A) and (C), respectively. Average values ± SD of three independent experiments are shown. (E and F) Western blot analyses of the solubilized supernatants from the cells expressing *N*-glycan-deficient mutants (E) and the W1 + W2 transfectants cultured with [TN(+)] or without tunicamycin [TN(−)] (F). Closed triangles indicate the migration positions of fully glycosylated POMT1 and POMT2. Open triangles indicate the migration positions of POMTs that have no *N*-glycan chains. Molecular weight standards are shown on the right. The mock lanes were loaded with sample from cells transfected with vector only, indicating endogenous POMT activity of HEK293 cells.

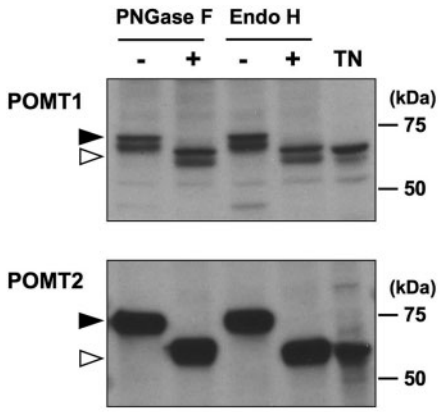

Fig. 5 Endo-glycosidase digestions of POMT1 and POMT2. The microsomal fractions from the W1 + W2 transfectants were treated with PNGase F or Endo H. Lane TN, microsomal fraction from the W1 + W2 transfectant cultured with tunicamycin. Closed triangles indicate the migration positions of fully glycosylated POMT1 and POMT2. Open triangles indicate the migration positions of the deglycosylated forms of POMT1 and POMT2. Molecular weight standards are shown on the right.

prevent Pmt1–Pmt2 interactions (*19*). Together, these results suggest that the loop 5s of human POMT1 and POMT2 do not have an important role in complex formation. We previously showed that POMT1 mutants derived from WWS patients could form a complex with wild-type POMT2, although these complexes did not have any POMT activity (*14*). Taken together, these results indicate that complex formation of POMT1–POMT2 is necessary but not sufficient for enzymatic activity.

Another question is when the POMT1–POMT2 complex is formed. We previously showed that POMT1 and POMT2 could not associate when they were expressed individually in different cells and then mixed (*1*). This suggests that the POMT1–POMT2 complex is formed concomitantly with translation in the ER. Further studies are needed to clarify the mechanism and role of complex formation and enzymatic activity. However, the present results show that *N*-glycosylation is needed for the correct folding of proteins and for enzymatic activity.

In the PMTs of *S. cerevisiae* and *Mycobacterium tuberculosis*, loop 1 was found to have a role in both enzymatic activity and complex formation (*19*, *26*). In POMT2, loop 1 may also contribute to activity because the activity of the N98Q transfectant (which lacks the *N*-glycan on Asn^{98} on loop 1) was lower than the activities of the wildtype and other mutants (Fig. 3D).

Yeast PMTs and human POMTs are predicted to be integral membrane proteins and have similar topologies with multiple transmembrane domains. However, there are some differences. For example, Triton X-100 appeared to abolish human POMT activity (*15*) but did not inhibit yeast PMT activity (*27*). The difference in detergent sensitivities may be due to differences in the amino acid sequences of POMTs and PMTs and in the lipid compositions of the ER membranes of humans and yeast. In addition, it has recently been reported that *O*-mannosylation of human POMTs requires a specific amino acid sequence while yeast *O*-mannosylation does not (*28*). This is consistent with the fact that *O*-mannosylation of proteins is common in yeast but rare in mammals. Differences in amino acid sequences and differences in the numbers, positions and structures of *N*-glycans between POMTs and PMTs may cause the difference of the substrate specificity of both. Further studies are necessary to elucidate the regulatory mechanism of protein *O*-mannosylation.

Funding

This study was supported by a Grant-in-Aid for Scientific Research (20370053, 19790244) from the Japan Society for the Promotion of Science, a Research Grant (20B-13) for Nervous and Mental Disorders and a Research on Psychiatric and Neurological Diseases and Mental Health (H20-016) from the Ministry of Health, Labor and Welfare of Japan and a Grant from The Takeda Science Foundation.

Conflict of interest

None declared.

References

1. Manya, H., Chiba, A., Yoshida, A., Wang, X., Chiba, Y., Jigami, Y., Margolis, R.U., and Endo, T. (2004) Demonstration of mammalian protein *O*-mannosyltransferase activity: coexpression of POMT1 and POMT2 required for enzymatic activity. *Proc. Natl Acad. Sci. USA* **101**, 500–505
2. Beltran-Valero De Bernabe, D., Currier, S., Steinbrecher, A., Celli, J., Van Beusekom, E., Van Der Zwaag, B., Kayserili, H., Merlini, L., Chitayat, D., Dobyns, W.B., Cormand, B., Lehesjoki, A.E., Cruces, J., Voit, T., Walsh, C.A., Van Bokhoven, H., and Brunner, H.G. (2002) Mutations in the *O*-Mannosyltransferase gene POMT1 give rise to the severe neuronal migration disorder Walker-Warburg syndrome. *Am. J. Hum. Genet.* **71**, 1033–1043
3. van Reeuwijk, J., Janssen, M., van den Elzen, C., Beltran-Valero de Bernabe, D., Sabatelli, P., Merlini, L., Boon, M., Scheffer, H., Brockington, M., Muntoni, F., Huynen, M.A., Verrips, A., Walsh, C.A., Barth, P.G., Brunner, H.G., and van Bokhoven, H. (2005) POMT2 mutations cause α-dystroglycan hypoglycosylation and Walker-Warburg syndrome. *J. Med. Genet.* **42**, 907–912
4. Chiba, A., Matsumura, K., Yamada, H., Inazu, T., Shimizu, T., Kusunoki, S., Kanazawa, I., Kobata, A., and Endo, T. (1997) Structures of sialylated *O*-linked oligosaccharides of bovine peripheral nerve α-dystroglycan. The role of a novel O-mannosyl-type oligosaccharide in the binding of α-dystroglycan with laminin. *J. Biol. Chem.* **272**, 2156–2162
5. Endo, T. (2004) Structure, function and pathology of *O*-mannosyl glycans. *Glycoconj. J.* **21**, 3–7
6. Muntoni, F., Brockington, M., Blake, D.J., Torelli, S., and Brown, S. C. (2002) Defective glycosylation in muscular dystrophy. *Lancet* **360**, 1419–1421
7. Michele, D.E. and Campbell, K.P. (2003) Dystrophin-glycoprotein complex: post-translational processing and dystroglycan function. *J. Biol. Chem.* **278**, 15457–15460
8. Brancaccio, A., Schulthess, T., Gesemann, M., and Engel, J. (1995) Electron microscopic evidence for a

mucin-like region in chick muscle α-dystroglycan. *FEBS Lett*. **368**, 139–142
9. Brancaccio, A., Schulthess, T., Gesemann, M., and Engel, J. (1997) The N-terminal region of α-dystroglycan is an autonomous globular domain. *Eur. J. Biochem*. **246**, 166–172
10. Kanagawa, M., Saito, F., Kunz, S., Yoshida-Moriguchi, T., Barresi, R., Kobayashi, Y.M., Muschler, J., Dumanski, J.P., Michele, D.E., Oldstone, M.B., and Campbell, K.P. (2004) Molecular recognition by LARGE is essential for expression of functional dystroglycan. *Cell* **117**, 953–964
11. Yamada, H., Chiba, A., Endo, T., Kobata, A., Anderson, L.V., Hori, H., Fukuta-Ohi, H., Kanazawa, I., Campbell, K.P., Shimizu, T., and Matsumura, K. (1996) Characterization of dystroglycan-laminin interaction in peripheral nerve. *J. Neurochem*. **66**, 1518–1524
12. Endo, T. (2005) Aberrant glycosylation of α-dystroglycan and congenital muscular dystrophies. *Acta. Myol*. **24**, 64–69
13. Manya, H., Bouchet, C., Yanagisawa, A., Vuillaumier-Barrot, S., Quijano-Roy, S., Suzuki, Y., Maugenre, S., Richard, P., Inazu, T., Merlini, L., Romero, N.B., Leturcq, F., Bezier, I., Topaloglu, H., Estournet, B., Seta, N., Endo, T., and Guicheney, P. (2008) Protein *O*-mannosyltransferase activities in lymphoblasts from patients with α-dystroglycanopathies. *Neuromuscul. Disord*. **18**, 45–51
14. Akasaka-Manya, K., Manya, H., and Endo, T. (2004) Mutations of the POMT1 gene found in patients with Walker-Warburg syndrome lead to a defect of protein *O*-mannosylation. *Biochem. Biophys. Res. Commun*. **325**, 75–79
15. Akasaka-Manya, K., Manya, H., Nakajima, A., Kawakita, M., and Endo, T. (2006) Physical and functional association of human protein *O*-mannosyltransferases 1 and 2. *J. Biol. Chem*. **281**, 19339–19345
16. Strahl-Bolsinger, S., Gentzsch, M., and Tanner, W. (1999) Protein *O*-mannosylation. *Biochim. Biophys. Acta*. **1426**, 297–307
17. Strahl-Bolsinger, S. and Scheinost, A. (1999) Transmembrane topology of pmt1p, a member of an evolutionarily conserved family of protein *O*-mannosyltransferases. *J. Biol. Chem*. **274**, 9068–9075
18. Girrbach, V. and Strahl, S. (2003) Members of the evolutionarily conserved PMT family of protein *O*-Mannosyltransferases form distinct protein complexes among themselves. *J. Biol. Chem*. **278**, 12554–12562
19. Girrbach, V., Zeller, T., Priesmeier, M., and Strahl-Bolsinger, S. (2000) Structure-function analysis of the dolichyl phosphate-mannose: protein *O*-mannosyltransferase ScPmt1p. *J. Biol. Chem*. **275**, 19288–19296
20. Hirokawa, T., Boon-Chieng, S., and Mitaku, S. (1998) SOSUI: classification and secondary structure prediction system for membrane proteins. *Bioinformatics* **14**, 378–379
21. Hofmann, K. and Stoffel, W. (1993) TMbase - a database of membrane spanning proteins segments. *Biol. Chem. Hoppe-Seyler* **374**, 166
22. Tusnady, G.E. and Simon, I. (2001) The HMMTOP transmembrane topology prediction server. *Bioinformatics* **17**, 849–850
23. Nilsson, I.M. and von Heijne, G. (1993) Determination of the distance between the oligosaccharyltransferase active site and the endoplasmic reticulum membrane. *J. Biol. Chem*. **268**, 5798–5801
24. Kobata, A. (1979) Use of endo- and exoglycosidases for structural studies of glycoconjugates. *Anal. Biochem*. **100**, 1–14
25. Trimble, R.B. and Maley, F. (1984) Optimizing hydrolysis of *N*-linked high-mannose oligosaccharides by endo-β-*N*-acetylglucosaminidase H. *Anal. Biochem*. **141**, 515–522
26. VanderVen, B.C., Harder, J.D., Crick, D.C., and Belisle, J.T. (2005) Export-mediated assembly of mycobacterial glycoproteins parallels eukaryotic pathways. *Science* **309**, 941–943
27. Strahl-Bolsinger, S. and Tanner, W. (1991) Protein *O*-glycosylation in Saccharomyces cerevisiae. Purification and characterization of the dolichyl-phosphate-D-mannose-protein *O*-D-mannosyltransferase. *Eur. J. Biochem*. **196**, 185–190
28. Manya, H., Suzuki, T., Akasaka-Manya, K., Ishida, H.K., Mizuno, M., Suzuki, Y., Inazu, T., Dohmae, N., and Endo, T. (2007) Regulation of mammalian protein *O*-mannosylation: preferential amino acid sequence for *O*-mannose modification. *J. Biol. Chem*. **282**, 20200–20206